J. Plasma Fusion Res. SERIES, Vol. 2 (1999) 414–417

Simulation of Various Ionization Effects in Overdense Plasmas Irradiated by a Subpicosecond Pulse Laser

ZHIDKOV Alexei, SASAKI Akira and TAJIMA Toshiki
Advanced Photon Research Center, Japan Atomic Energy Research Institute, Neyagawa, 572, Japan

(Received: 9 December 1998 / Accepted: 22 June 1999)

Abstract

The effects of the elastic collisions and ionization under non-LTE on the absorption efficiency, heat transfer, and particle acceleration in short pulse laser irradiated overdense plasmas are studied. We present a newly developed hybrid electromagnetic particle-in-cell method (in 1D) employing the nonlinear Langevin equation to account for Coulomb collisions and the average ion model to calculate the plasma transient ionization. The collisional and field ionization are included. Interaction between solid targets and thin foils with an arbitrary polarized, intense ($I = 10^{16}$–10^{20}W/cm^2) laser pulse are investigated

Keywords:
PIC, Langevin equation, average ion model, field ionization

1. Introduction

The interaction of an intense, short pulse laser with an overdense plasma plays a pivotal role in various aspects ranging from basic research such as laboratory astrophysics and high field science to practical applications including development of X-ray sources and particle accelerators. We study the effects of the elastic collisions and ionization under non-LTE on the absorption efficiency, heat transfer, and particle acceleration in short pulse laser irradiated plasmas. We present a newly developed hybrid electromagnetic particle-in-cell method employing the nonlinear Langevin equation to account for Coulomb collisions and the average ion model for the non-LTE ionization balance. The effect of field ionization are included along with collisional ionization. To explore the absorption of an obliquely incident p-polarized pulse a two wave approximation (TWA) for the Maxwellian curl equations [1] is employed.

2. General Equation

We have developed a hybrid PIC code combined with atomic kinetics calculation on kinetics cells. A kinetics cell includes many PIC cells and is used for plasma parameters calculation. To solve the Fokker-Planck equation in the frame of PIC simulation we have to use the Langevin equation for motion of charged particles. For plasma electrons the equation has a following dimensionless form,

$$\frac{d\boldsymbol{v}}{dt} = -[\boldsymbol{E}(\boldsymbol{r}) + \boldsymbol{v}\times\boldsymbol{H}(\boldsymbol{r})] - \gamma\frac{m_e}{M}\frac{Z^2\boldsymbol{v}}{v^3} + \sqrt{\frac{\gamma Z^2}{v}}\left(\boldsymbol{\varsigma} - \frac{\boldsymbol{v}(\boldsymbol{v}\boldsymbol{\varsigma})}{v^2}\right) - 2\gamma Z\frac{\boldsymbol{u}I_p(u)}{u^3} + \sqrt{\frac{\gamma Z}{u}}\left\{\sqrt{I_p(u) + \frac{2}{3}uI_s(u) - \frac{1}{3u^2}I_E(u)}\left[\boldsymbol{\xi} + \boldsymbol{\eta} - \frac{\boldsymbol{u}}{u^2}(\boldsymbol{u}, \boldsymbol{\xi} + \boldsymbol{\eta})\right]\right.$$

Corresponding author's e-mail: zhidkov@apr.jaeri.go.jp

$$+\sqrt{\frac{2}{3}uI_s(u)+\frac{2}{3u^2}I_E(u)}\,\frac{u}{u^2}(u,\xi-\eta)\Bigg\},$$

$$\gamma=4\pi\Lambda\left(\frac{e^2}{m_e c^2}\right)^2\frac{cN_i}{\omega},\quad u=(v-\bar{u})/<v>,$$

$$\bar{u}=\sum v,\quad <v>=\sqrt{\frac{2}{3N}\sum(v-\bar{u})^2},$$

$$I_p(v)=\int_0^v f(z)z^2dz,\quad I_p(\infty)=1,$$

$$I_E(v)=\int_0^v f(z)z^4dz,\quad I_s(v)=\int_v^\infty f(z)z\,dz. \qquad (1)$$

In Eq. (1), Z, N_i, M are the ion charge, density, and mass, N is the number of particle in a kinetics cell [1]. f(v) is the advanced distribution function of plasma electrons in a kinetics cell, ω is the laser frequency. η, ζ, ξ describe the normal random processes [1]. The time in (1) is measured in ω^{-1}, the fields in $(e/mc\omega)^{-1}$, velocity in c.

The Maxwellian equations in the frame of the TWA, to incorporate the oblique incidence, can be written as following [1],

$$\frac{\partial}{\partial x}A_\pm \pm \sin\theta\frac{\partial}{\partial\tau}A_\pm =$$

$$-\frac{1}{2}j_Y\sin\theta\mp\frac{1}{2}\cos\theta\left(j_X+\frac{\partial E_{ST,X}}{\partial\tau}\right),$$

$$H_Z=(A_++A_-)/\sin\theta,\quad E_{L,Y}=A_+-A_-,$$

$$E_X=E_{L,X}+E_{ST,X},\quad E_{L,X}=(A_++A_-)\cos\theta/\sin\theta, \qquad (2)$$

where j is the plasma current, $E_{st,x}$, E_L plasma and laser electric fields, θ the incident angle, $\theta = \pi/2$ is the normal incidence. The collisional absorption, vacuum heating, anomalous skin effect, and resonance absorption can be calculated by Eq. (2) [1].

We include the transient ionization in the frame of the average ion model by allowing change in the charge of superparticles in PIC simulation. The charge change is calculated by the balance equation,

$$\frac{dQ_{ek}}{dt}=N_Z\left[-Q_{ek}\left(R_Z N_e\right)+\sum_{e_1>I_Z}q_1 v_1\sigma_Z(v_1)\right.$$

$$\left.+\frac{\alpha}{\tau(I_{z+1},E_k)}\right], \qquad (3)$$

where Q_{ek} is the total charge of electron superparticles (q_1) in a kinetic cell, R_z is the recombination rate, σ_z is the cross-section for collisional ionization, τ is a probability of the field ionization, E_k is the electric field, I_z is the ionization potential, α is a constant. The charge change obtained from solution of Eq. (3) is redistributed over all particles in a kinetics cell.

3. Results of Calculation

Figure 1 represents a comparison between the results of simulations using the present PIC method with Langevin equation and the direct solution of the Fokker-Planck equation [2] for a solid carbon plasma irradiated by KrF laser pulse of 0.3 ps duration and intensity $I = 10^{16}$W/cm^2. In such a plasma collisions dominate the absorption and the heat transfer. A good agreement in the heat transfer and variable ionization shows the ability of the presented method.

Figure 2 illustrates the effect of the return current on the heat transfer and plasma ionization when the absorption is dominated by collsionless processes such as the resonance absorption and vacuum heating. When intense p-polarized pulse laser irradiates the target, the high energy electrons are produced from variety of interaction as direct acceleration by the laser field or after resonant excitation of plasma waves. The return current arises to compensate the charge separation in the plasma when the fast electron penetrates into the plasma. The absorbed energy is deposited near the plasma surface due to the collisional process-Ohmic heating caused by the return current. Having less energy than the fast electrons, the electrons from the return current ionize plasma more efficiently. The transient ionization results in the change of the plasma conductivity and energy deposition. Electron- electron collisions increase the plasma conductivity and runaway rate, which subsequently change the heat penetration depth and ionization near the plasma surface because these collisions dominate the energetic part of the distribution of the return current electrons.

The expansion of a thin metallic foil irradiated by an intense picosecond p-polarized pulse laser resembles evaporation process. The fast electrons produce the electrostatic field on the plasma surfaces. The multiply charged ions are accelerated by this field to very high energy and finally considerable portion of the absorbed energy is utilized to the kinetic energy of fast ions, while the plasma bulk has relatively low temperature. The temporal evolution of the absorption efficiency for Al foil of 125nm irradiated by 1 ps, p-polarized (45°) pulse Ti-Saf laser of $I = 4 \times 10^{16}$W/cm^2 is presented in Fig. 3 for the collisional (a) and collisionless (b) plasmas. The evolution is similar for the both cases. Initially, the absorption is steered by the vacuum heating, and collisions in the case (a). As ion are accelerated, and the scale length of the plasma is

increased, the absorption increases due to the resonance absorption. When the resonance absorption becomes dominant the energy of the plasma waves is transformed directly to the ion acceleration. The energy utilized for ion acceleration is about 25% of laser's for both cases while the energies of the plasma electrons and waves are different. By changing ion charges the transient ionization dominates entire process. Figure 4 presents the ion charge distribution in a carbon foil of 200nm thickness irradiated by intense, $I = 4 \times 10^{19}$W/cm^2, Ti-Saf laser pulse with normal (a) and oblique, 45°, (b) incidence for 80 fs. The calculation has been carried out without elastic collisions. The field and collisional ionization have been included. If we consider only collisional ionization the pulse duration is too short for efficient ionization. In this case there is no efficient ion

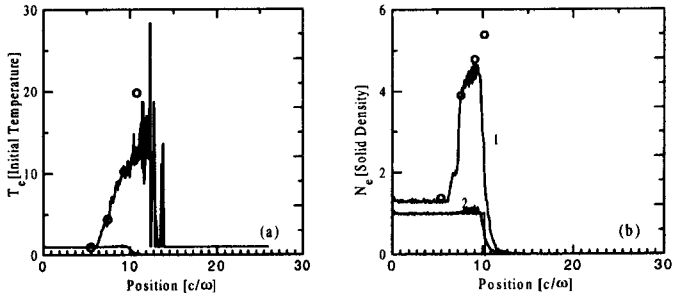

Fig.1 A good agreement between calculated electron temperature (a) and density (b) distribution in a solid carbon plasma after laser pulse $t = 0.3$ps (KrF, intensity $I = 10^{16}$W/cm^2, normally incident) obtained by PIC & Langevin simulation (curves) and by direct solution of the FP equation [2] (circles). (1) - electron, (2) - ion density. $T_0 = 20$eV.

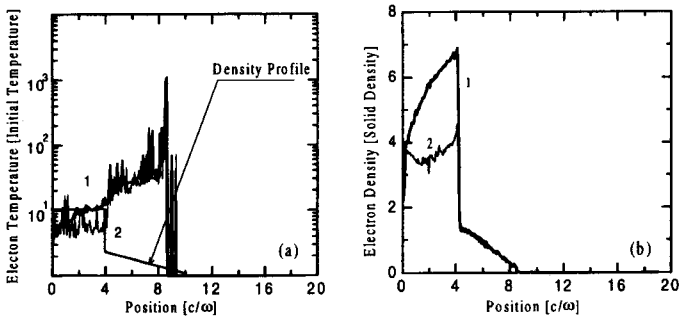

Fig. 2 Effect of the return current on the heat transfer and ionization in a solid Si plasma irradiated by a p-polarized pulse laser with $\lambda = 800$nm, $I = 4 \times 10^{16}$W/cm^2, $\theta = 45°$. The resonance absorption is dominant. (1) e-e and e-i collisions, (2) only e-i collisions. $T_0 = 10$eV.

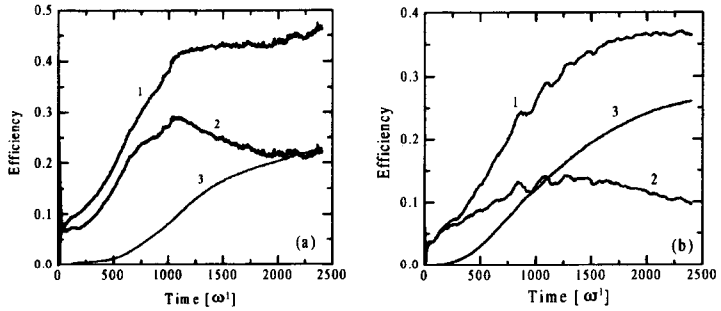

Fig. 3 Absorption efficiency (1) of an 800nm, 1ps pulse laser by Al foil of 125nm with elastic collisions (a) and without (b). $I = 4 \times 10^{16}$W/cm^2. (2) energy utilized for electron heating and plasma waves, (3) energy utilized for ion acceleration.

acceleration. If only OFI is added there is only backward ion acceleration. The skin layer is much less than the foil thickness and there is no laser field on opposite foil surface. But fast electrons produced by the ponderomotive force create the strong electric field there. For such high intensity, in spite of being less than the laser field, this electrostatic field can be strong enough for rapid field ionization

The distribution of ion velocities are shown in Fig. 5. For low intensity, after t = 0.5ps, multiply charged ions from the plasma surfaces are accelerated over 1MeV while the electron energies are $1/Z$ as much as the ion's, where Z is the ion charge. For high intensity, due to the field ionization, ions are accelerated over 10MeV in the both sides. Because of the direct acceleration of plasma electrons by the laser field there is no essential difference in the forward acceleration between plasmas irradiated by the normally or obliquely incident pulses.

4. Conclusion

It is found that the effect of ionization and elastic collisions change the heat front penetration in solid targets irradiated by obliquely incident laser pulses. This is because those effects cause significant change of the plasma conductivity and, as a result, heat transfer due to the fast electrons. The efficient ionization is produced by electrons from the return current. The Ohmic heating due to the return current is responsible to the energy deposition.

Plasma expansion during one picosecond p-polarized pulse laser resembles an evaporation process. An essential portion (half) of the absorbed energy is utilized for ion acceleration. Multiply charged ions are accelerated from the plasma surfaces over 1MeV energy by the plasma electrostatic field even at comparably low laser intensities. As the ion charge increases during transient ionization, ions are accele- rated to higher energies. At higher intensity the plasma ionization is dominated by the laser and plasma fields. The ionization by plasma electrostatic field has significant effect on the forward ion acceleration from thin foil plasmas.

References

[1] A. Zhidkov and A. Sasaki, JAERI-Report 98-068 (1998).

[2] R.P. Town, A.R. Bell and S.J. Rose, Phys. Rev. Lett. **74**, 924 (1995).

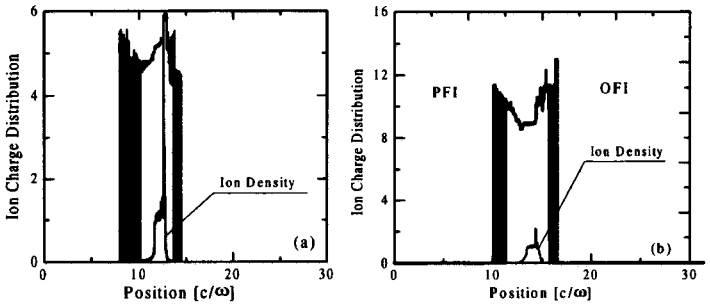

Fig. 4 Spatial distribution of charges of ions accelerated from foils of 200nm thickness by a λ = 800nm, $I = 4 \times 10^{19}$W/cm^2, normally incident pulse laser after t = 80fs, (a) carbon and (b) aluminum.

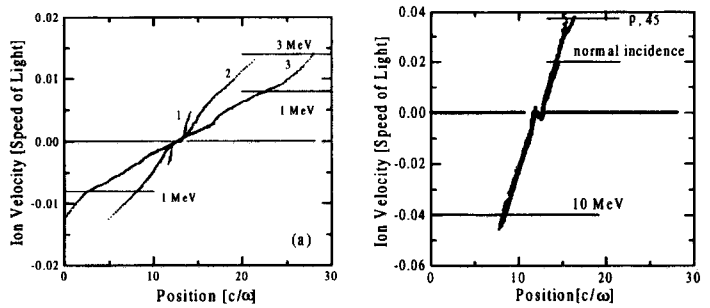

Fig. 5 Spatial distribution of ion velocities in (a) Al (see, Fig.3) and (b) in C (see, Fig.4) foils; a: (1) t = 0.1ps, (2) t = 0.5ps, (3) t = 1ps, b: after t = 80fs.